Published in final edited form as:

Oncogene. 2016 January 21; 35(3): 377–388. doi:10.1038/onc.2015.95.

NAG-1/GDF15 Accumulates in the nucleus and modulates transcriptional regulation of the Smad pathway

K-W Min[1,*], **JL Liggett**[1], **G Silva**[1], **WW Wu**[2], **R Wang**[2], **R-F Shen**[2], **TE Eling**[3], and **SJ Baek**[1]

[1]Department of Biomedical and Diagnostic Sciences, College of Veterinary Medicine, University of Tennessee, Knoxville, TN 37996, USA

[2]Facility for Biotechnology Resources, CBER, Food and Drug Administration, Bethesda, MD 20892, USA

[3]Laboratory of Molecular Carcinogenesis, NIH/NIEHS, Research Triangle Park, NC 27709, USA

Abstract

Protein dynamics, modifications, and trafficking are all processes that can modulate protein activity. Accumulating evidence strongly suggests that many proteins play distinctive roles dependent on cellular location. Nonsteroidal anti-inflammatory drug activated gene-1 (NAG-1) is a TGF-β superfamily protein that plays a role in cancer, obesity, and inflammation. NAG-1 is synthesized and cleaved into a mature peptide, which is ultimately secreted into the extracellular matrix (ECM). In this study, we have found that full-length NAG-1 is expressed in not only the cytoplasm and ECM, but also in the nucleus. NAG-1 is dynamically moved to the nucleus, exported into cytoplasm, and further transported into the ECM. We have also found that nuclear NAG-1 contributes to inhibition of the Smad pathway by interrupting the Smad complex. Overall, our study indicates that NAG-1 is localized in the nucleus and provides new evidence that NAG-1 controls transcriptional regulation in the Smad pathway.

Keywords

NAG-1; GDF-15; TGF-beta; Smad

INTRODUCTION

The study of genes altered by anti-cancer compounds has great value in regard to cancer chemoprevention and therapeutics. Building on this research, we identified the non-steroidal anti-inflammatory drug (NSAID)-activated gene-1 (*NAG-1*) as a divergent member of the TGF-β superfamily.[1] *NAG-1* has also been identified by other groups using a variety of

Correspondence: Seung Joon Baek, PhD, Department of Biomedical and Diagnostic Sciences, College of Veterinary Medicine, University of Tennessee, 2407 River Drive, Knoxville, TN 37996-4542, Tel: +1 865 974 8216;, Fax: +1 865 974 5616, ; Email: sbaek2@utk.edu

[*]**Current Address:** Department of Cell and Molecular Pharmacology, Medical University of South Carolina, Charleston, SC 29425

CONFLICT OF INTEREST

The authors declare that they have no conflict of interest.

different cloning strategies and has been called *growth differentiation factor 15 (GDF15),*[2] *placental transformation growth factor-β (PTGFB*),[3] *macrophage inhibitory cytokine-1 (MIC-1),*[4] *prostate-derived factor (PDF),*[5] and *placental bone morphogenetic protein (PLAB).*[6] Research to date has demonstrated that NAG-1 is able to be induced not only by NSAIDs,[7] but also by chemopreventive dietary compounds[8–12] and PPARγ ligands.[13–16] These compounds affect NAG-1 induction via the tumor suppressor genes p53, early growth response-1 (EGR-1), and/or via the PI3K/AKT/GSK-3β pathway.[13, 17–19] Unlike the transcriptional regulation of NAG-1, the principal function, receptor, and signaling pathway of NAG-1 remain uncertain, and the biological role of NAG-1 in tumorigenesis remains poorly understood and sometimes contradictory. For example, NAG-1 plays a role in cancer development and progression, but various results show it acting as either a pro-tumorigenic or anti-tumorigenic protein.[20] NAG-1 also controls stress responses, bone formation, hematopoietic development, and adipose tissue function, as well as contributing to cardiovascular diseases.[21–23]

Our group has developed a transgenic mouse that ubiquitously over-expresses the human *NAG-1* gene.[24] These mice are resistant to chemical- and genetic-induced cancers and have a decreased systemic inflammatory response.[21, 24, 25] Furthermore, the transgenic mice weigh less and have less fat, despite similar food intake as wild-type (WT) littermates, suggesting NAG-1 may act to alter metabolism as well.[24] Recently, we reported that NAG-1 modulates metabolic activity by increasing the expression of key thermogenic and lipolytic genes in adipose tissue.[26] That study suggested that NAG-1 is also a novel therapeutic target in preventing and treating obesity and insulin resistance.

NAG-1 is synthesized as a 308-amino acid pro-NAG-1 monomer and then dimerizes by a specific disulfide linkage. The pro-NAG-1 dimer is then cleaved by furin-like proteases at an RXXR site, forming a 112 amino acid C-terminal dimeric protein and pro-peptide.[20] This mature dimeric protein is secreted into the ECM, and can be detected in the blood of humans. Some evidence suggests the pro-NAG-1 dimer binds to the ECM and contributes to latent storage in the stroma,[27] but the fate and role of pro-NAG-1 is poorly understood. Experimental evidence clearly confirms the secreted mature dimer has biological activity;[26] however, the multiple forms of NAG-1 present in the cells, their interaction with the cellular system, and their biological activity is unclear. Therefore, there is clearly a need for further study of the molecular mechanisms by which pro-NAG-1 contributes to NAG-1's biological activity.

A number of studies suggest that secreted proteins can localize in the nucleus and exhibit distinctive activity.[28, 29] For example, secreted proteins bFGF and odontogenic ameloblast-associated protein (ODAM) are expressed in the nucleus and cytoplasm, as well as the ECM.[30] Thus, a secreted protein like NAG-1 could also localize and alter molecular events within the nucleus. In this report, we tested this hypothesis and show the trans-localization of pro-NAG-1 into the nucleus followed by its exportation by CRM1.

TGF-β is a strong epithelial-mesenchymal transition (EMT) inducer, and substantial studies established crucial roles of TGF-β-induced EMT in tumor progression.[31] EMT enhances cellular migration and invasion properties, as cell migration required loss of cell-cell

contacts and acquisition of mesenchymal characteristics[32]. In addition, TGF-β regulates the expression and secretion of matrix metalloproteinase 2 (MMP2) and MMP9, and the modulations of the extracellular structure is required for tumor angiogenesis. Thus, TGF-β contributes to enabling tumor cells to invade normal tissues and metastasize to distant organs.

Our results suggest that the cleavage of pro-NAG-1 to the mature form and its subsequent secretion is dependent on translocation into the nucleus. The pro-NAG-1 inside the nucleus altered gene expression and interfered with the TGF-β1-induced Smad signaling pathway, thereby altering cell migration. This is the first study demonstrating the critical importance of NAG-1 nuclear translocation in secretion of the mature dimer and the first report confirming a biological activity for pro-NAG-1 in the nucleus.

RESULTS

Full-length wild-type NAG-1 (pro-NAG-1) translocates to the nucleus

Because emerging evidence suggests that proteins exhibit distinctive activities based on cellular location, we decided to examine whether NAG-1 protein is located in different cellular regions. NAG-1 is first formed as pro-NAG-1 and then cleaved into a pro-peptide and a mature dimer form, which is then secreted into circulation. To investigate the cellular location of NAG-1 and the secretion events, we first used U2OS stable cell lines in which pro-NAG-1 is induced by treatment with tetracycline.[33] Only the pro-NAG-1 was present inside the cells with no mature form observed (Figure 1a). Interestingly, nuclear/cytoplasmic fractionation of U2OS cells demonstrated that pro-NAG-1 was equally expressed in both the cytoplasm and the nucleus in U2OS cells (Figure 1b). Lamin A/C and tubulin α were used as controls for nuclear and cytoplasmic fractions, respectively. To confirm our finding, we constructed expression vectors for GFP- and V5/His-tagged NAG-1 and conducted an immunofluorescence assay to observe subcellular localization of NAG-1 in U2OS cells transiently transfected with the NAG-1/GFP expression vector. NAG-1 signal (green) was observed in both the nucleus and the cytoplasm with a considerable signal in the ER/Golgi region (Figure 1c). NAG-1 seemed to be localized in nucleolus; however, NAG-1 expression was not confined to nucleolus, as shown in a co-localization experiment with fibrillarin, a marker for nucleolus expression (Supplementary Figure S1a). To define the location of NAG-1 in more detail, we performed subcellular fractionation, which separates cell components into soluble cytoplasmic extract (CE), membrane extract (ME), soluble nuclear extract (NE), and chromatin-bound protein extract (CB). As shown in Figure 1d, pro-NAG-1 was expressed in both ME and NE fractions. Cell lysates from *tet*-inducible system and wild-type U2OS cells transiently transfected with the pNAG-1/V5/His expression vector were separated into components. The phenomenon of finding pro-NAG-1 in nuclear fractions is observed both in the transient and stable NAG-1 expressing cells. Endogenous NAG-1 expression is induced by treatment with several anti-cancer compounds in HCT-116 human colorectal cancer cells.[34] As shown in Figure 1e, HCT-116 cells incubated with anticancer compounds for 24 h express endogenous pro-NAG-1 in nucleus, suggesting a rapid translocation into the nucleus. A confocal microscopy analysis supports our finding that NAG-1 is present in the nucleus (Supplementary Figure S1b). Overall, pro-NAG-1 is

surprisingly expressed in the nucleus in addition to the membrane fractions, including the vesicle and ER/Golgi apparatus.

NAG-1 may contain a non-canonical nuclear localization signal domain and is imported to the nucleus via the nuclear pore complex

Since NAG-1 does not contain the classical nuclear localization signal (NLS), two independent programs were used to search for the non-classical NLS.[35, 36] Both programs found one potential non-classical NLS (aa 190-197). Another potential NLS (aa 211-218) was selected by only one program. Subsequently, two deletion mutant clones (Δ190-197 and Δ211-218) from the NAG-1/V5/His expression vector were generated (Figure 2a) and expressed in wild-type U2OS and HCT-116 cells. Nuclear/cytoplasmic localization showed that the expression level of the two NAG-1 mutants was higher in the cytoplasmic fraction than in the nucleus, in both cell types (Figure 2a). These data are further confirmed by subcellular fractionation, indicating that Δ190-197 NAG-1 has less NAG-1 expression in the nuclear extraction (Supplementary Figure S2a). Thus, these mutant NAG-1 proteins are still translocated into the nucleus but at a much lower amount, compared to wild-type NAG-1. These results were confirmed by immunofluorescence analysis with NAG-1/GFP construct, indicating that less signal intensity of mutant NAG-1-transfected cells was observed in the nucleus, compared to wild-type NAG-1-transfected cells (Figure 2b). Thus, these two regions, aa 190-197 and aa 211-218, may contribute, at least in part, to translocation of NAG-1 protein from the cytoplasm to the nucleus. It has been reported that a protein can have multiple NLS that may function cooperatively to affect efficient nuclear transport.[37, 38] Since two putative NLS sites exhibit a marginal effect on nuclear entry of NAG-1, serial deletion mutant clones were generated to address this issue. As shown in Figure 2c, none of clones resulted in a higher ratio of cytoplasmic NAG-1 to nuclear NAG-1. However, the expression of one NAG-1 mutant clone (Δ2-29 clone) interestingly resulted in predominant expression in the nucleus (Figure 2c). To determine whether this translocation requires energy and/or the nuclear pore complex, an in vitro nuclear import assay was performed using NAG-1/GFP fusion proteins. Permeabilized cells lose their transport systems; therefore, cytosolic extract and the ATP/GTP regenerating system were provided to investigate nuclear uptake of NAG-1/GFP. As shown in Figure 2d, NAG-1/GFP protein localized in the nucleus, whereas GFP protein alone did not. These results suggest that NAG-1/GFP does not enter the nucleus by a simple diffusion pathway because of the large size of the NAG-1/GFP protein (more than 60 kDa), and that ATP is required to transport NAG-1 into the nucleus. In addition, inactivation of the nuclear pore complex (NPC) by wheat germ agglutinin (WGA) abolished NAG-1 movement to the nucleus. Since the secreted NAG-1 cannot be absorbed by the cells (Supplementary Figure S2b), only cytoplasmic NAG-1 is subjected to nuclear entry. Taken together, these results indicate that the nuclear entry of NAG-1 is energy-dependent via the nuclear pore complex, and those two sites (190-197 and 211-218), in part, contribute to the nuclear entry of NAG-1.

NAG-1 has a canonical nuclear export signal (NES) mediated by CRM1

Next, we decided to further analyze the 2-29 region of NAG-1, as shown in Figure 2c, in terms of nuclear accumulation of NAG-1. We generated more deletion clones within this region and found that the Δ14-29 clone contains a domain to control predominantly nuclear

accumulation of NAG-1 (Supplementary Figure S3a, b). We also generated a glycosylation site mutant clone (N70A) because it has been known that glycosylation sites may affect nuclear translocation of proteins[39]. This clone showed an expression pattern of NAG-1 similar to that of wild-type (Supplementary Figure S3a). As shown in Figure 3a, the Δ14-29 clone exhibited higher expression of NAG-1 in the nucleus (lane 3 vs 7). As a control, we transfected an R193A mutant clone that cannot be cleaved at the RXXR site, and wherein mature NAG-1 cannot be secreted. To elucidate if the Δ14-29 mutant clone altered secretion of the mature form, conditioned medium from the same batch used in Figure 3a was purified, and secreted mature NAG-1 was measured by Western blot analysis. As expected, both pro-NAG-1 and mature NAG-1 (Figure 3b, lane 2) were detected in pNAG-1/V5 transfected medium, while the R193A clone secreted only the pro-NAG-1 (Figure 3b, lane 4). However, we could not detect Δ14-29 pro-NAG-1 nor mature NAG-1 in the culture medium (Figure 3b, lane 3). These data indicate that the Δ14-29 region is necessary for exporting pro-NAG-1 protein to the cytoplasm from the nucleus and thus no mature NAG-1 is present in the media.

Our results also indicate a putative NES sequence in the Δ14-29 region.[36] Therefore, two mutants (ΔNES and mutNES) were generated to investigate whether the Δ14-29 region plays a role in nuclear exportation of NAG-1 (Figure 3c). The expression pattern of NAG-1 in U2OS cells with a ΔNES or mutNES construct showed essentially nucleus expression with little to no cytoplasm expression in contrast with the wild-type NAG-1 control (Figure 3c and Supplementary S4a). Confirmation of nuclear expression was obtained with immunofluorescence of U2OS cells transfected with pNAG/ΔNES/V5 and pNAG/mutNES/V5 constructs (Figure 3d). Chromosome region maintenance 1 (CRM1; also referred to as exportin1 or Xpo1) is a key protein in exporting a protein from the nucleus into the cytoplasm.[40] To determine whether CRM1 is involved in NAG-1 exportation, we added the CRM1 inhibitor leptomycin B (LMB) to the cells to see nuclear retention of NAG-1. The pro-NAG-1 nuclear distribution was increased in the cells treated with LMB in a dose-dependent manner (Supplementary Figure 4b, c and d). Smad4 was used as a control because it is regulated by CRM1 in exportation out of the nucleus[41]. Finally, we conducted an immunoprecipitation assay to determine whether pro-NAG-1 physically interacts with CRM1. As shown in Figure 3e, pro-NAG-1 was indeed immunoprecipitated with CRM1, suggesting that NAG-1 exportation to the cytoplasm is controlled by CRM1. There is a possibility that the 14-29 aa region of NAG-1 may have signal sequences for direct secretion to the extracellular region in addition to those for exportation from the nucleus. To address this possibility, we observed the level of NAG-1 secretion after LBM treatment. As expected, LMB treatment blocked NAG-1 secretion, suggesting that the 14-29 aa region is not only for exportation from the nucleus but also for secretion (Figure 3f). To further support the evidence that an NES exists in NAG-1, we employed the interspecies heterokaryon assay (Supplementary S4e), the results of which suggested that NAG-1 shuttles between the nucleus and the cytoplasm, and LMB treatment blocks nucleocytoplasmic shuttling properties of NAG-1.

RNA-seq analysis suggests that NAG-1 inhibits the expression of TGF-β target genes

To date, little is known about the NAG-1 receptor and its downstream pathways. Transcriptome sequencing (RNA-seq) is a promising tool in elucidating downstream effects and/or pathways. To study the effects and downstream pathways of NAG-1, we employed comparative RNA-seq profiling of the transcriptomes using U2OS and *tet*-induced U2OS cells. RNA-seq results revealed 142 differentially expressed genes (Figure 4a). Nineteen of the 142 genes were previously reported to be a potential TGF-β target gene with regard to their relative abundance presented in the heat map (Figure 4b). Ingenuity network analysis was used to identify possible interactions with other genes differentially expressed in our dataset, and suggested NAG-1 expression reduced the expression of several TGF-β1-related genes (Figure 4c). Although we did not treat the cells with TGF-β1 for RNA-seq experiments, U2OS cells exhibited basal level of p-Samd2/3 without exogenous TGF-β1 treatment (Supplementary Figure S5). We selected 10 out of 19 genes because they are well-known Smad target genes and confirmed their expression in the cells transfected with pNAG-1/His/V5 expression vector by qRT-PCR (Figure 4d). Except for HMGA1, the expression of NAG-1 inhibited the expression of these downstream targets of TGF-β1, suggesting pro-NAG-1 acts as an inhibitor of the TGF-β1 pathway. To examine further the effect of pro-NAG-1 on the TGF-β signaling pathway, two promoter reporters, *p3TP-Luc* and *pPAI-800-Luc,* were transfected with NAG-1 expression vector into U2OS and HEK293 cells, which are responsible for TGF-β treatment. NAG-1 expression diminished TGF-β1-mediated Smad activities (p3TP-Luc and pPAI-800-Luc) (Figure 4e). Thus, pro-NAG-1 expression inhibits the TGF-β1-mediated Smad signaling pathway at the transcriptional level.

Nuclear NAG-1 mitigates TGF-β signaling via interrupting Smads to DNA binding

To address to what extent NAG-1 is relevant to endogenous Smad target genes, we treated the cells with TGF-β1 and measured the expression of the known TGF-β target genes *SERPINE1, TIMP3, and LTBP1*. Gene expression was suppressed in the presence of NAG-1 and further suppressed in the presence of ΔNES-NAG-1, which is in agreement with a higher level of nuclear pro-NAG-1 (Figure 5a). In U2OS and MCF10A cells (TGF-β-responding cells), wild-type NAG-1 and mutNES NAG-1 expression inhibited the Smad pathway, as assessed by Smad binding element (SBE) reporter activity (Figure 5b). Similar results were observed in MCF7 cells using *p3TP* and *PAI-1* reporters (Supplementary Figure S6a). Expression of the R193A mutant, which does not produce the mature NAG-1, also inhibited TGF-β-mediated Smad transcriptional activity (Supplementary Figure S6b), supporting the hypothesis that pro-NAG-1, but not mature NAG-1, is involved in the inhibition of Smad signaling.

To further investigate how NAG-1 modulates the TGF-β1 response, we measured the level of phosphorylation of Smad2 in the presence of TGF-β1. Wild-type U2OS cells were transfected with either empty or NAG-1 expression vector and then treated with TGF-β1. After 1 h, the media were aspirated and fresh media were added. The cells were then harvested in a time course for Western blot analysis. Pro-NAG-1 did not affect Smad2 phosphorylation (Figure 5c), suggesting that upon TGF-β1 stimulation, NAG-1 inhibits TGF-β1 signaling without inhibiting phosphorylation of Smad2. To examine if pro-NAG-1

affects the translocation of Smad2 to the nucleus and Smad2 degradation, the distribution of Smad2 was investigated. As shown in Figure 5d, Smad2 distribution was the same in both cytosol (lanes 1, 2 vs 3, 4) and the nucleus (lanes 6, 7 vs 8, 9), regardless of whether NAG-1 was present. Furthermore, this result was confirmed using A549 cells that were transfected with either LacZ or ΔNES NAG-1, and the distribution of Smad2 between cytosol and nucleus was examined (Supplementary Figure S6c). Thus, pro-NAG-1 did not affect Smad2 translocation into the nucleus upon TGF-β1 stimulation or Smad2 degradation. We next explored whether the DNA-binding activity of Smad was diminished by NAG-1 expression. The DNA pull-down assay indicated that SBE binding activity of the Smad complex was diminished when NAG-1 was expressed, implying that NAG-1 may interrupt Smad DNA-binding activity in the nuclear region (Figure 5e, Supplementary Figure S6d). Furthermore, a ChIP assay showed that NAG-1 inhibits binding of Smad to the promoter region of TGF-β target genes (Figure 5f). Taken together, these results suggest that nuclear pro-NAG-1 attenuates TGF-β-mediated Smad signaling through interruption of DNA binding activity of the Smad complex upon TGF-β1 stimulation.

NAG-1 Attenuates TGF-β-induced cell migration

TGF-β1 is a cytokine that increases cell migration and invasion.[42] We next examined if NAG-1 expression altered TGF-β1-induced cell migration. As shown in Figure 6a, NAG-1 expression diminished cell migration into the scratched region in response to TGF-β1. In addition, a trans-well migration assay showed less migration in the NAG-1- or mutNES-NAG-1-expressing cells in comparison to the empty vector-transfected cells (Figure 6b). We employed a 3D culture system to study invasion. Spheroids composed of empty vector-transfected cells exhibited spindle-like protrusions after TGF-β1 treatment; however, spheroids composed of WT-expressing or mutNES-expressing cells did not (Figure 6c). NAG-1 also suppressed expression of snail1 and slug, which are markers for epithelial–mesenchymal transition (EMT) induced by TGF-β1 (Supplementary Figure S7). Overall, NAG-1 expression appeared to suppress EMT and cell invasion activity of TGF-β1 by inhibiting Smad DNA-binding activity.

DISCUSSION

Multiple cellular localizations of protein give rise to multiple functions or integrate signals from different locations to fulfill one biological outcome.[43, 44] NAG-1 is a secreted TGF-β superfamily member, and plays a role as a cytokine to affect several biological activities through an unknown receptor. While working on cellular NAG-1 movement, we discovered that NAG-1 is significantly expressed in the nucleus and affects transcriptional regulation of the Smad complex. NAG-1 expression is altered by a variety of signals, such as those from cytokines (IL-1β, TNF-α, macrophage colony-stimulating factor),[4] radiation,[3] tissue injury,[45] anoxia,[46] and many chemopreventive/chemotherapeutic chemicals,[47] suggesting NAG-1 signaling may be important for maintaining cellular homeostasis. In addition, NAG-1 is a target gene of several transcription factors, such as p53,[3, 48] NF-κB,[49] Sp1,[1] and Egr-1.[13] However, downstream signaling pathways affected by NAG-1 remain to be discovered.

Although *in vitro* assays show different results, the results from NAG-1 over-expression in NAG-Tg mice and NAG-1 depletion in NAG-1 knockout mice consistently support the notion for anti-tumorigenic activity.[24, 25, 50] Some possible explanations for the contradictory activity of NAG-1 *in vitro* include: 1) NAG-1's different functions in the different cancer types, 2) an unidentified role of pro-NAG-1 in cells, and 3) the contribution of NAG-1 binding proteins or receptors in different cells. In fact, there are many examples of other proteins having dual biological functions in different cancer types and microenvironments. For example, EGR-1 has been shown to be associated with pro-tumorigenic activity in prostate cancer,[51] whereas EGR-1 acts like a tumor suppressor protein in other cancers.[52] 15-lipooxygenase-1 (LOX-1) is another example; LOX-1 acts as a tumor suppressor in colorectal cancer and a pro-tumorigenic protein in prostate cancer.[53, 54] Thus, the fact that NAG-1 shows dual functions in carcinogenesis is not surprising. Lack of knowledge of NAG-1's receptor and/or binding proteins is a large hurdle to studying its signaling pathway; however, a couple of reports have suggested that NAG-1 may be involved in TGF-β receptor-mediated signaling.[3, 55] Based on our data, we were surprised to find that NAG-1 expressed in the nucleus, and that nuclear NAG-1 inhibited the formation of the TGF-β1-induced Smad/DNA complex formation, thereby inhibiting expression of Smad target genes. This observation consistently occurred in other cells, and our data suggest that inhibition of the Smad pathway by the nuclear NAG-1 expression may provide a new avenue to support NAG-1's role in anti-tumorigenesis. However, there is a dichotomy view that NAG-1 could positively affect to tumor development in where TGF-β exerts as a tumor suppressor protein because TGF-β signaling is a complex web that target genes and biological consequences of TGF-β could be dictated by contextual determinants such as signal transduction, transcription and epigenetic status.[42]

Our results also suggest that NAG-1 could translocate into the nucleus through an active transport system (Figure 2d); however, we have yet to define the precise mechanisms involved in its nuclear importation. It is likely that multiple pathways or a novel pathway may affect NAG-1 movement to the nucleus since two potential mutations partially affected NAG-1 importation (Figure 2a and b). We also made a double mutation clone at Δ190-197 and Δ211-218, and found that this clone exhibited a similar pattern as the single mutation clone (data not shown). Since no canonical NLS signals were found in the NAG-1 full-length peptide sequences, NAG-1 may have a unique mechanism that is able to translocate it into the nucleus. NAG-1 has two putative SUMOylation sites at C-terminal region (http://www.abgent.com/tools). SUMOylation could also exert for nuclear localization of NAG-1.[56] Thus, it is possible that SUMOylation of NAG-1 may affect nuclear translocation when the two NLS sites in NAG-1 are disrupted. The TGF-β superfamily member BMP2 has been observed in a truncated form in the nucleus;[57] however, the current study is the first report that a full-length TGF-β superfamily protein is expressed in the nucleus and plays a role in transcription. Nuclear importation of NAG-1 requires energy and carrier proteins. GFP by itself was not able to enter nuclei (Figure 2d); however, NAG-1/GFP was imported into the nucleus as examined by an *in vitro* import assay. Depleting the energy generation system and NPC inhibitor WGA treatment in the permeabilized cells reduced nuclear uptake of NAG-1, suggesting that NAG-1 nuclear entry occurs through the NPC in an energy-dependent manner. Given that NAG-1 lacks a classical NLS region and requires the NPC for

translocation, nuclear localization of NAG-1 likely requires interaction with a partner that contains the NLS domain.[58] Indeed, nuclear importation of protein can be mediated by multiple transport receptors,[37, 38] or a protein containing armadillo repeats can directly interact with a component of nuclear pore proteins.[59] Thus, it is likely that a portion of NAG-1 is exposed to the cytoplasm while another portion of NAG-1 is embedded in ER/Golgi for being recognized by a transporter, as seen in EGFR nuclear importation.[60] Although we have not ruled out these possibilities, our data indicate that two sites (190-197 and 211-218) play a role, at least in part, in importing NAG-1 to the nucleus. Further experiments are necessary to define the molecular mechanism of nuclear transport and specifically, the exact component of import machinery for NAG-1.

In comparison to the importation mechanism of NAG-1, we were able to investigate in greater detail NAG-1 exportation to the cytoplasm. NAG-1 export was mediated by an LMB-sensitive, CRM1-dependent pathway, which requires a functional domain to be recognized by CRM1. Sequence analysis showed that the canonical, leucine-rich NES was present within the N-terminal region of NAG-1. If this site were deleted or mutated, then NAG-1 was retained in the nucleus of the cells. We also observed that NAG-1 physically bound to CRM1; however, we cannot exclude the possibility that other nuclear proteins that supply NES may help NAG-1 exportation. Interestingly, we could not find secreted mature NAG-1 in the culture medium when NAG-1 was retained in the nucleus. It is likely that one of the secretion pathways of NAG-1 must pass through the nucleus prior to processing to the mature form. Vesicles are required for NAG-1 secretion, and the vesicle containing NAG-1 may form at the nuclear membrane; therefore, an NES sequence may play a pivotal role in vesicle formation. Indeed, our results show that NAG-1 is localized in the ER/Golgi region in the cytoplasm, not as a soluble cytosolic fraction (Figure 1d) and that this localization is dependent upon sequences in the N-terminal domain, a region that contains an NES sequence (Figure 3c). Notably, there is a possibility that anti-tumorigenic activity of NAG-1 may occur with nuclear NAG-1, whereas secreted mature NAG-1 protein may possess pro-tumorigenic activity. This is supported by previous reports indicating that recombinant NAG-1 increases kinase pathways in some cancer cells.[61] Although further mechanistic studies are required to define the exact biological activity of nuclear NAG-1 and secreted mature NAG-1, our data clearly show that nuclear NAG-1 causes inhibition of cell migration and invasion mediated by TGF-β1, as assessed by experiments with mutant clones. Based on our data and that in the literature, it is postulated that more nuclear NAG-1 will be expressed in cells that need anti-tumorigenic status, whereas more secreted NAG-1 will be expressed in pro-tumorigenic status.

The biological role of NAG-1 nuclear-cytoplasmic shuttling remains to be established. In this study, we found that nuclear NAG-1 could control the strength of TGF-β1-mediated Smad signaling. It remains to be clarified how nuclear NAG-1 modulates the DNA binding capacity of the Smad complex, even though it has been known that various factors and cellular context attenuate Smad-mediated transcription. One possible way is that NAG-1 might bind directly to DNA (SBE) to compete with Smad, although no DNA binding motif has been identified in the NAG-1 sequence. To test this hypothesis, we employed ChIP-seq to see if any DNA fragments were pulled down with NAG-1. It is not likely that NAG-1 directly binds to conserved SBE, since we have not identified any genes related to the SBE-

containing promoter. Another possibility is that NAG-1 may bind to Smad2, thereby inhibiting Smad binding activity. However, we could not find any direct physical interaction between Samd2/3/4 and NAG-1 (Supplementary Figure S8). Our data rather imply that NAG-1 somehow interrupts the Smad complex in the nucleus by an unknown mechanism(s). Smad proteins may need an additional transcription factor or co-factor to strongly occupy their target DNA.[62, 63] Thus, NAG-1 might disrupt the formation of the Smad complex upon TGF-β1 stimulation, or NAG-1 might somehow facilitate ADP-ribosylation, which dissociates the Smad complex from DNA, leading to attenuation of a Smad-specific gene response.[64] Another possible explanation is that NAG-1 may affect phosphorylation sites in the hinge region by nuclear protein CDK8/9.[65] This facilitates Smad protein binding to another DNA-binding co-factor, which is required for proper transcription of TGF-beta target genes. Thus, it is likely that many pathways are additively involved in interrupting the Smad complex by NAG-1 expression.

Our data show that all cells tested tended to express NAG-1 in varying amounts in both the cytoplasm and nucleus (Figure 3a). This provides a model that could demonstrate strategies for therapeutic intervention in disease states in which “inappropriate” localization of protein is believed to contribute to disease development.[66] It remains to be elucidated whether more transformed tumor cells activate mechanisms that allow increased nuclear import or decreased nuclear export of NAG-1. We are currently developing an antibody that recognizes the N-terminal region of NAG-1 to examine NAG-1 expression in the nucleus of human tissue samples and to determine whether more nuclear staining of NAG-1 is associated with a better prognosis in cancer patients.

In summary, our data indicate that the pro-NAG-1 was expressed in the nucleus and appears to play a role in transcriptional regulation by disturbing the Smad complex. In addition, nuclear retention resulted in an absence of secreted mature NAG-1. The schematic diagram in Figure 6d represents the proposed model of the molecular mechanism of nuclear-cytoplasmic NAG-1 shuttling through active transport and nuclear NAG-1, attenuating TGF-β signaling through interruption of DNA binding of the Smad complex upon TGF-β stimulation. In addition, the novel role of NAG-1 in the nucleus may help lead to the development of new drugs that facilitate the retention of NAG-1 in the nucleus or to the development of novel diagnostic tools for assessing cancer progression.

MATERIALS AND METHODS

Cell culture and reagents

U2OS and HCT-116 were cultured in McCoy’s 5A supplemented with 10% FBS (Hyclone) and 1% penicillin/streptomycin (Lonza). HEK293 cells were cultured in Dulbecco’s modified Eagle’s medium (DMEM) with 10% FBS and 1% penicillin/streptomycin. The NAG-1 tetracycline-inducible U2OS cell line has been described previously[33]. All cultured cells were maintained at 37°C in humid conditions with 5% CO_2. The following antibodies were purchased from Santa Cruz Biotechnology (Santa Cruz, CA, USA): anti-V5 (sc-271944), anti-CRM1 (sc-5595), anti-tubulin α (sc-8035), anti-lamin A/C (sc-6215), anti-histone H1 (sc-10806), anti-β-actin (sc-47778) and anti-GFP (sc-9996). Anti-Smad2 (#5339), anti-phosphor-smad2 (#3108), anti-smad2/3 (#8685), anti-phosphor-smad2/3

(#8828), anti-smad4 (#9515), anti-snail (#3879), anti-slug (#9585), anti-hsp90 (#4877) and anti-calnexin (#2679) were purchased from Cell Signaling (Danvers, MA, USA). Recombinant human TGF-β1 (#8915) was also purchased from Cell Signaling. CRM1 inhibitor (leptomycin B, L-6100) was from LC Laboratories (Woburn, MA, USA).

DNA Constructs and transfection

Full-length NAG-1 PCR product amplified from pcDNA3/NAG-1[34] was sub-cloned into pcDNA3.1/V5/His-TOPO vector (Invitrogen, Carlsbad, CA, USA) and pcDNA3.1/CT-GFP-TOPO vector (Invitrogen) to generate the V5/His- and GFP-tagged clones, respectively. All mutant constructs were generated from pNAG1-V5/His or pNAG1-GFP using the QuickChange II site-directed Mutagenesis Kit (Stratagene, Santa Clara, CA, USA). PCR primer sequences are described in Supplemental Table 1, and all DNA constructs used were verified by DNA sequencing. Transient transfections were carried out using either PolyJet (SignaGen, Gaithersburg, MD, USA) or TransIT-2020 transfection reagent (Mirus Bio, Madison, WI, USA) according to the manufacturer's protocol.

Luciferase assay

Cells were seeded on a 12-well plated at a density of 1.0×10^5 cells/well. TGF-β1-inducible reporter constructs *p3TP-luc*, *pPAI-800-luc* (*SERPINE1* promoter), and *pSBE4-luc* were each co-transfected with *pRL-null* vector. After 24 h transfection, cells were stimulated with TGF-β1 for 24 h in serum-free conditions, and then were harvested in 1 x passive lysis buffer (Promega, Madison, WI, USA). Luciferase activity was examined using a DualGlo Luciferase Assay Kit (Promega), and data were normalized by pRL-null luciferase activity.

Subcellular fractionation and immunofluorescence

For subcellular fractionation, either a Nuclear Extract Kit (Active Motif, Carlsbad, CA, USA) or Subcellular Protein Fractionation Kit (Thermo Scientific, Waltham, MA, USA) was used according to the manufacturer's protocol. Proteins for each fraction were subjected to Western blot analysis. For immunofluorescence, cells were plated on a glass bottom culture dish (MatTek, Ashland, MA, USA). After transient transfection, cells were washed twice with phosphate-buffered saline (PBS) and fixed with 4% paraformaldehyde for 15 min. After two PBS washes, cells were permeabilized with PBS containing 0.25% Triton X-100 for 10 min, followed by incubating with 1% bovine serum albumin in PBS for 30 min to block non-specific binding of the antibodies. The cells were incubated with diluted primary antibody overnight followed by incubation with FITC-conjugated secondary antibody (610-602-002, Rockland Immunochemicals, Gilbertsville, PA, USA) for 1 h in the dark. After counterstaining with DAPI, fluorescence was observed at 400 x magnification, with digital enlargement when required.

Western blot and immunoprecipitation

For Western blot, reduced protein samples lysed by RIPA buffer were separated on 8% or 10% SDS-PAGE gels, and transferred to nitrocellulose membranes (Osmonics). The membranes were incubated with a specific primary antibody in TBS containing 0.05% Tween 20 (TSB-T) and 5% nonfat dry milk at 4°C overnight. After three washes with TBS-

T, the blots were incubated with horseradish peroxidase-conjugated IgG for 1 h at room temperature, visualized using detection reagent (Thermo Scientific), and quantified by Scion Image Software (Scion Corp.). To conduct immunoprecipitation analysis, 1 mg of cell extract lysed by modified RIPA buffer (25 mM Tris-Cl pH7.4, 150 mM NaCl, 1 % NP-40, and 5 % glycerol) was incubated with 2 μg primary antibody for 2 h at 4°C on a rotating platform, followed by adding protein A/G PLUS-agarose (Santa Cruz) overnight. Immunoprecipitation was collected by centrifuge at 1000x*g* for 3 min. After washing five times with modified RIPA buffer, the pellets were resuspended with 50 μL 2XSDS-PAGE sample loading buffer and heated at 95°C for 5 min. Western blot analysis was conducted as described above using 20 μL of the immunoprecipitated samples.

In vitro nuclear import assay

HCT-116 cells were plated on glass coverslips 24 h prior to use. The cells were rinsed three times with transport buffer (TB; 20 mM HEPES, pH 7.3, 110 mM potassium acetate, 2 mM magnesium acetate), and permeabilized for 5 min with complete TB containing 1 mM EGTA, 2 mM DTT, 1 mM PMSF, protease inhibitor cocktail, and 30 μg/mL digitonin on ice. After two washes with TB, the permeabilized cells were incubated in complete TB with HCT-116 cytosol extract, the appropriate GFP-tagged NAG-1 expressed in *in vitro* TNT Quick Coupled Transcription/Translation Systems (Promega), and an ATP regeneration system (0.5 mM ATP and GTP, 5 mM creatine phosphate, and 50 μg/mL creatine kinase). Assays in the absence of an energy-regenerating system were conducted with TB without the ATP regeneration system. For WGA treatments, permeabilized cells were incubated in the presence of 0.05 mg/mL WGA in TB for 15 min prior to the import reaction. After the import assay, cells were fixed with 4% paraformaldehyde, and fluorescent proteins were analyzed by immunofluorescence assay.

Library preparation and next generation sequencing (NGS)

Inducible U2OS cells were grown in the presence or absence of tetracycline (2 μg/mL) for 2 days. Total RNAs were isolated using E.Z.N.A Total RNA Kit (Omega Bio-Tek, Norcross, GA, USA) following the manufacturer's protocol. An Illumina TruSeq RNA kit (V2; San Diego, CA, USA) was used for library preparation of mRNA-Seq according to the vendor's instruction. Briefly, (poly A+) mRNAs were purified from 1 μg total RNA using poly-T magnetic beads. Messenger RNAs were fragmented to desired lengths by incubating at an elevated temperature (94°C) for 8 min in the presence of metal ions. The RNAs were used as templates for the syntheses of the first- and second-strand cDNAs, which were subsequently subjected to end repair, A-tailing at 3′ ends, adapter ligation, and 15-cycle PCR amplifications. During PCR, individual barcodes were incorporated into respective samples to enable sample pooling in subsequent DNA sequencing. Paired-end 100-cycle sequencing of the prepared RNA-Seq libraries were performed on an Illumina HiSeq 2500, following standard protocols of the manufacturer.

NGS Data analysis

Sequence reads were processed using the Tuxedo suite (Baltimore, MD, USA).[67] Briefly, fastq files were aligned to the UCSC human reference genome (hg19) using the TopHat v. 2.0.6 software program. The aligned reads were then assembled by Cufflinks v.2.0.2 to

produce individual transcripts, followed by Cuffmerge to integrate the reference human genome annotation (GTF transcription annotations from Illumina iGenomes). The output files were then passed onto the Cuffdiff program to create differential expression results.

Real-time qRT-PCR

Total RNA was isolated using an E.Z.N.A Total RNA Kit (Omega Bio-Tek) according to the manufacturer's protocol. Complementary DNA was made from 1 μg isolated RNA using a Verso cDNA synthesis kit (Thermo Scientific) according to the manufacturer's protocol. PCR was carried out using iTaq Universal SYBR Green Supermix (Bio-Rad, Hercules, CA, USA). Primers used for qRT-PCR are provided in Supplementary Table 3. Relative quantities of mRNAs were calculated using the $\Delta\Delta C_t$ method and normalized using human Ribosomal Protein, Large, P0 (RPLP0) as an endogenous control.

Scratch and transwell migration assay

For the scratch migration assay, inducible U2OS cells were plated onto a 6-well plate and cultured to near (> 90%) confluence. Cells were serum starved for 24 h in the presence or absence of 2 μg/mL tetracycline, and the monolayer was scratched with a sterile 10 μL-pipette tip. Then serum-free media containing 10 ng/mL of TGF-β1 was added for 24 h. Phase-contrast images were acquired at 0 and 24 h after the gaps were created. The cells migrated into the gaps were counted from three different gap regions. For the transwell migration assay, transfected U2OS cells were resuspended in serum-free medium, and the cell suspension (4×10^4 cells) was added to the upper transwell chamber (pore size of 8 μM; Costar; Corning, Corning, NY, USA). Media containing 0.1% serum and TGF-β1 was added to the bottom wells of the chambers. Cells were incubated for 18 h at 37°C, fixed with 4% paraformaldehyde, and permeabilized by 100% methanol. Cells were then stained with 0.5% crystal violet dissolved in 20% methanol at room temperature for 15 min. Cells that had not migrated after 18 h were removed from the upper face of the filters using cotton swabs. Migrated cells were counted under a light microscope. Images of three different fields were taken for each membrane.

3D spheroid invasion assay

A 96-well 3D spheroid BME cell invasion assay kit (Cultrex) was used according to the manufacturer's protocol with minor modification. Briefly, 2,000 cells were resuspended in serum-free media containing spheroid formation ECM. The cells were added to a 96-well ultralow attachment round bottom plate, and then incubated for 1 day to allow cells to assemble into compact spheroids. Invasion matrix was added to each well, and then the cells were incubated for 1 h prior to adding serum-free media containing 10 ng/mL TGF-β1. The plate was incubated for 2 days, and spheroids were photographed at 8 x magnification.

DNA pull-down assay

Tetracycline-treated or non-tetracycline-treated inducible U2OS cells grown on a 10-cm dish were stimulated with or without 5 ng/mL of TGF-β1 for 2 h. Whole cell lysates were prepared in lysis buffer (10 mM HEPES pH 7.5, 150 mM NaCl, 1 mM MgCl2, 0.5 mM EDTA, 0.5 mM DTT, 0.1% NP-40, 10% glycerol). Lysates were centrifuged at 4°C for 15

min at high speed. Cell lysate (500 μg) was incubated with 5 μg poly(dI-dC) and 1 μg biotinylated SBE oligonucleotides containing Smad binding elements at 4°C for 16 h. DNA-bound proteins were collected with streptavidin beads (G-Biosciences, St. Louis, MO, USA) for 2 h. Beads were collected by centrifugation for 30 s at 3000 *g* and washed four times with lysis buffer. Then, 2Xsample buffer (50 μL) was added to the beads and boiled for 5 min, followed by Western blotting. The SBE probe sequence for DNA pull-down was Biotine-5′-TCGATAGCCAG-ACAGGTAGCCAGACAGGTAGCCAGACAGGTAGCCAGACAGG-3′[68].

Chromatin immunoprecipitation

For the chromatin immunoprecipitation assay, a MAGnify chromatin immunoprecipitation system (Invitrogen) was used according to the manufacturer's protocol. Briefly, cells were grown to 70~80% confluence in a 150-mm dish. The cells were crosslinked with 1% formaldehyde for 10 min at room temperature. Crosslinking reactions were quenched with 0.125 M glycine for 5 min at room temperature. The cells were scraped and moved to a 1.5-mL tube, then sonicated for 8 cycles of 15 s on/1 min off. Sheared chromatin was incubated with either Smad2/3 antibody or normal IgG conjugated with beads for 2 h at 4°C. Chromatin-bound DNA was reverse cross-linked and DNA was purified. Purified DNA was subjected to qRT-PCR using the following primer pairs: TIMP3 promoter region, forward 5′-GCAAACAGCAGATGGCTTCC -3′ and reverse 5′-CCTTGACTGTGCTTGGTGGA - 3′; SMAD7 promoter region, forward 5′-TTCTGGGAGCTTCTCTGCCC -3′ and reverse 5′-GCTCCGGCCTCGTCAC -3′.

Interspecies heterokaryon assay

The human U2OS cells grown in glass bottom dishes were transiently transfected with the pNAG-1/V5/His expression vector. At 24 h post transfection, the U2OS cells were washed with PBS twice, and then an equal number of murine NIH3T3 cells were seeded onto the same glass bottom dishes. After 6 h incubation, cycloheximide (CHX, 100 μg/ml) and 10 nM LMB were added to inhibit protein synthesis and nuclear export of a protein. The co-cultured cells were washed twice with PBS after 2 h and were added with polyethylene glycol MW 8000 (PEG) 50% (w/v) in PBS for 2 min to allow cell fusion, followed by washing twice with serum-free medium containing CHX. The cells were then incubated with complete media (plus CHX along with LMB) for 1 h. After fixation in 4% paraformaldehyde, the cells were counterstained with Hoechst 33258 to distinguish human U2OS nuclei from those of murine NIH3T3 cells.

Statistical analysis

Statistical analysis was performed with the Student unpaired *t* test. Results were considered statistically significance at $*P < 0.05$, $**P < 0.01$ and $***P < 0.001$.

Supplementary Material

Refer to Web version on PubMed Central for supplementary material.

Acknowledgments

We thank Dr. Xingya Wang (College of Pharmaceutical Science, Zhejiang Chinese Medical University, China) and Ms. Misty Bailey (University of Tennessee) for their critical reading of this manuscript. We also thank Dr. John Dunlap (Advanced Microscopy and Imaging Center at The University of Tennessee) for providing technical help on confocal microscopy. This work was supported by the National Institutes of Health (R01CA108975), and the Center of Excellence in Livestock Diseases and Human Health, University of Tennessee, to S.J.B. This research was also supported, in part, by the NIH, NIEHS Intramural Research Program (T.E.E) Z01- ES010016-14.

References

1. Baek SJ, Horowitz JM, Eling TE. Molecular cloning and characterization of human nonsteroidal anti-inflammatory drug-activated gene promoter. Basal transcription is mediated by Sp1 and Sp3. J Biol Chem. 2001; 276:33384–33392. [PubMed: 11445565]
2. Bottner M, Laaff M, Schechinger B, Rappold G, Unsicker K, Suter-Crazzolara C. Characterization of the rat, mouse, and human genes of growth/differentiation factor-15/macrophage inhibiting cytokine-1 (GDF-15/MIC-1). Gene. 1999; 237:105–111. [PubMed: 10524241]
3. Li PX, Wong J, Ayed A, Ngo D, Brade AM, Arrowsmith C, et al. Placental transforming growth factor-beta is a downstream mediator of the growth arrest and apoptotic response of tumor cells to DNA damage and p53 overexpression. J Biol Chem. 2000; 275:20127–20135. [PubMed: 10777512]
4. Bootcov MR, Bauskin AR, Valenzuela SM, Moore AG, Bansal M, He XY, et al. MIC-1, a novel macrophage inhibitory cytokine, is a divergent member of the TGF-beta superfamily. Proc Natl Acad Sci U S A. 1997; 94:11514–11519. [PubMed: 9326641]
5. Paralkar VM, Vail AL, Grasser WA, Brown TA, Xu H, Vukicevic S, et al. Cloning and characterization of a novel member of the transforming growth factor-beta/bone morphogenetic protein family. J Biol Chem. 1998; 273:13760–13767. [PubMed: 9593718]
6. Hromas R, Hufford M, Sutton J, Xu D, Li Y, Lu L. PLAB, a novel placental bone morphogenetic protein. Biochim Biophys ACTA. 1997; 1354:40–44. [PubMed: 9375789]
7. Baek SJ, Wilson LC, Lee CH, Eling TE. Dual function of nonsteroidal anti-inflammatory drugs (NSAIDs): inhibition of cyclooxygenase and induction of NSAID-activated gene. J Pharmacol Exp Ther. 2002; 301:1126–1131. [PubMed: 12023546]
8. Baek SJ, Kim JS, Jackson FR, Eling TE, McEntee MF, Lee SH. Epicatechin gallate-induced expression of NAG-1 is associated with growth inhibition and apoptosis in colon cancer cells. Carcinogenesis. 2004; 25:2425–2432. [PubMed: 15308587]
9. Lee SH, Cekanova M, Baek SJ. Multiple mechanisms are involved in 6-gingerol-induced cell growth arrest and apoptosis in human colorectal cancer cells. Mol Carcinog. 2008; 47:197–208. [PubMed: 18058799]
10. Lee SH, Kim JS, Yamaguchi K, Eling TE, Baek SJ. Indole-3-carbinol and 3,3′-diindolylmethane induce expression of NAG-1 in a p53-independent manner. Biochem Biophys Res Commun. 2005; 328:63–69. [PubMed: 15670751]
11. Lee SH, Yamaguchi K, Kim JS, Eling TE, Safe S, Park Y, et al. Conjugated linoleic acid stimulates an anti-tumorigenic protein NAG-1 in an isomer specific manner. Carcinogenesis. 2006; 27:972–981. [PubMed: 16286461]
12. Yang MH, Kim J, Khan IA, Walker LA, Khan SI. Nonsteroidal anti-inflammatory drug activated gene-1 (NAG-1) modulators from natural products as anti-cancer agents. Life Sci. 2014
13. Baek SJ, Kim JS, Nixon JB, DiAugustine RP, Eling TE. Expression of NAG-1, a transforming growth factor-beta superfamily member, by troglitazone requires the early growth response gene EGR-1. J Biol Chem. 2004; 279:6883–6892. [PubMed: 14662774]
14. Yamaguchi K, Cekanova M, McEntee MF, Yoon JH, Fischer SM, Renes IB, et al. Peroxisome proliferator-activated receptor ligand MCC-555 suppresses intestinal polyps in ApcMin/+ mice via extracellular signal-regulated kinase and peroxisome proliferator-activated receptor-dependent pathways. Mol Cancer Ther. 2008; 7:2779–2787. [PubMed: 18790758]
15. Min KW, Zhang X, Imchen T, Baek SJ. A peroxisome proliferator-activated receptor ligand MCC-555 imparts anti-proliferative response in pancreatic cancer cells by PPARgamma-

independent up-regulation of KLF4. Toxicol Appl Pharmacol. 2012; 263:225–232. [PubMed: 22750490]

16. Chintharlapalli S, Papineni S, Baek SJ, Liu S, Safe S. 1,1-Bis(3′-indolyl)-1-(p-substitutedphenyl)methanes are peroxisome proliferator-activated receptor gamma agonists but decrease HCT-116 colon cancer cell survival through receptor-independent activation of early growth response-1 and nonsteroidal anti-inflammatory drug-activated gene-1. Mol Pharmacol. 2005; 68:1782–1792. [PubMed: 16155208]
17. Baek SJ, Wilson LC, Hsi LC, Eling TE. Troglitazone, a peroxisome proliferator-activated receptor gamma (PPAR gamma) ligand, selectively induces the early growth response-1 gene independently of PPAR gamma. A novel mechanism for its anti-tumorigenic activity. J Biol Chem. 2003; 278:5845–5853. [PubMed: 12475986]
18. Lee S-H, Bahn JH, Choi CK, Whitlock NC, English AE, Safe S, et al. ESE-1/EGR-1 pathway plays a role in tolfenamic acid-induced apoptosis in colorectal cancer cells. Mol Cancer Ther. 2008; 7:3739–3750. [PubMed: 19074849]
19. Yamaguchi K, Lee SH, Eling TE, Baek SJ. Identification of nonsteroidal anti-inflammatory drug-activated gene (NAG-1) as a novel downstream target of phosphatidylinositol 3-kinase/AKT/GSK-3beta pathway. J Biol Chem. 2004; 279:49617–49623. [PubMed: 15377673]
20. Wang X, Baek SJ, Eling TE. The diverse roles of nonsteroidal anti-inflammatory drug activated gene (NAG-1/GDF15) in cancer. Biochem Pharmacol. 2013; 85:597–606. [PubMed: 23220538]
21. Kim JM, Kosak JP, Kim JK, Kissling G, Germolec DR, Zeldin DC, et al. NAG-1/GDF15 Transgenic Mouse Has Less White Adipose Tissue and a Reduced Inflammatory Response. Mediators Inflamm. 2013; 2013:641851. [PubMed: 23737651]
22. Johnen H, Kuffner T, Brown DA, Wu BJ, Stocker R, Breit SN. Increased expression of the TGF-b superfamily cytokine MIC-1/GDF15 protects ApoE(−/−) mice from the development of atherosclerosis. Cardiovasc Pathol. 2012; 6:499–505. [PubMed: 22386250]
23. Macia L, Tsai VW, Nguyen AD, Johnen H, Kuffner T, Shi YC, et al. Macrophage inhibitory cytokine 1 (MIC-1/GDF15) decreases food intake, body weight and improves glucose tolerance in mice on normal & obesogenic diets. PLoS ONE. 2012; 7:e34868. [PubMed: 22514681]
24. Baek SJ, Okazaki R, Lee SH, Martinez J, Kim JS, Yamaguchi K, et al. Nonsteroidal anti-inflammatory drug-activated gene-1 over expression in transgenic mice suppresses intestinal neoplasia. Gastroenterology. 2006; 131:1553–1560. [PubMed: 17101328]
25. Cekanova M, Lee SH, Donnell RL, Sukhthankar M, Eling TE, Fischer SM, et al. Nonsteroidal anti-inflammatory drug-activated gene-1 expression inhibits urethane-induced pulmonary tumorigenesis in transgenic mice. Cancer Prev Res (Phila). 2009; 2:450–458. [PubMed: 19401523]
26. Chrysovergis K, Wang X, Kosak J, Lee SH, Kim JS, Foley JF, et al. NAG-1/GDF-15 prevents obesity by increasing thermogenesis, lipolysis and oxidative metabolism. Int J Obes (Lond). 2014; 38:1555–1564. [PubMed: 24531647]
27. Bauskin AR, Brown DA, Junankar S, Rasiah KK, Eggleton S, Hunter M, et al. The propeptide mediates formation of stromal stores of PROMIC-1: role in determining prostate cancer outcome. Cancer Res. 2005; 65:2330–2336. [PubMed: 15781647]
28. Planque N. Nuclear trafficking of secreted factors and cell-surface receptors: new pathways to regulate cell proliferation and differentiation, and involvement in cancers. Cell Commun Signal. 2006; 4:7. [PubMed: 17049074]
29. Marchant DJ, Bellac CL, Moraes TJ, Wadsworth SJ, Dufour A, Butler GS, et al. A new transcriptional role for matrix metalloproteinase-12 in antiviral immunity. Nat Med. 2014; 20:497–506.
30. Lee H-K, Lee D-S, Ryoo H-M, Park J-T, Park S-J, Bae H-S, et al. The odontogenic ameloblast-associated protein (ODAM) cooperates with RUNX2 and modulates enamel mineralization via regulation of MMP-20. J Cell Biochem. 2010; 111:755–767. [PubMed: 20665536]
31. Ikushima H, Miyazono K. TGFβ signalling: a complex web in cancer progression. Nat Rev Cancer. 2010; 10:415–424. [PubMed: 20495575]
32. Akhurst RJ, Hata A. Targeting the TGF[beta] signalling pathway in disease. Nat Rev Drug Discov. 2012; 11:790–811. [PubMed: 23000686]

33. Baek SJ, Wilson LC, Eling TE. Resveratrol enhances the expression of non-steroidal anti-inflammatory drug-activated gene (NAG-1) by increasing the expression of p53. Carcinogenesis. 2002; 23:425–434. [PubMed: 11895857]
34. Baek SJ, Kim KS, Nixon JB, Wilson LC, Eling TE. Cyclooxygenase inhibitors regulate the expression of a TGF-beta superfamily member that has proapoptotic and antitumorigenic activities. Mol Pharmacol. 2001; 59:901–908. [PubMed: 11259636]
35. Nguyen Ba A, Pogoutse A, Provart N, Moses A. NLStradamus: a simple Hidden Markov Model for nuclear localization signal prediction. BMC Bioinformatics. 2009; 10:202. [PubMed: 19563654]
36. Kosugi S, Hasebe M, Tomita M, Yanagawa H. Systematic identification of cell cycle-dependent yeast nucleocytoplasmic shuttling proteins by prediction of composite motifs. Proc Natl Acad Sci U S A. 2009; 106:10171–10176. [PubMed: 19520826]
37. Theodore M, Kawai Y, Yang JQ, Kleshchenko Y, Reddy SP, Villalta F, et al. Multiple nuclear localization signals function in the nuclear import of the transcription factor Nrf2 (vol 283, pg 8984, 2008). J Biol Chem. 2008; 283:14176–14176.
38. Waldmann I, Walde S, Kehlenbach RH. Nuclear import of c-Jun is mediated by multiple transport receptors. J Biol Chem. 2007; 282:27685–27692. [PubMed: 17652081]
39. Chan CP, Mak TY, Chin KT, Ng IO, Jin DY. N-linked glycosylation is required for optimal proteolytic activation of membrane-bound transcription factor CREB-H. J Cell Sci. 2010; 123:1438–1448. [PubMed: 20356926]
40. Hutten S, Kehlenbach RH. CRM1-mediated nuclear export: to the pore and beyond. Trends Cell Biol. 2007; 17:193–201. [PubMed: 17317185]
41. Pierreux CE, Nicolás FJ, Hill CS. Transforming Growth Factor β-Independent Shuttling of Smad4 between the Cytoplasm and Nucleus. Mol Cell Biol. 2000; 20:9041–9054. [PubMed: 11074002]
42. Massague J. TGF[beta] signalling in context. Nat Rev Mol Cell Biol. 2012; 13:616–630. [PubMed: 22992590]
43. Sirover MA. Subcellular dynamics of multifunctional protein regulation: Mechanisms of GAPDH intracellular translocation. J Cell Biochem. 2012; 113:2193–2200. [PubMed: 22388977]
44. Kuo T-F, Tatsukawa H, Kojima S. New insights into the functions and localization of nuclear transglutaminase 2. FEBS J. 2011; 278:4756–4767. [PubMed: 22051117]
45. Zimmers TA, Jin X, Hsiao EC, McGrath SA, Esquela AF, Koniaris LG. Growth differentiation factor-15/macrophage inhibitory cytokine-1 induction after kidney and lung injury. Shock. 2005; 23:543–548. [PubMed: 15897808]
46. Albertoni M, Shaw PH, Nozaki M, Godard S, Tenan M, Hamou MF, et al. Anoxia induces macrophage inhibitory cytokine-1 (MIC-1) in glioblastoma cells independently of p53 and HIF-1. Oncogene. 2002; 21:4212–4219. [PubMed: 12082608]
47. Baek SJ, Eling TE. Changes in gene expression contribute to cancer prevention by COX inhibitors. Prog Lipid Res. 2006; 45:1–16. [PubMed: 16337272]
48. Tan M, Wang Y, Guan K, Sun Y. PTGF-beta, a type beta transforming growth factor (TGF-beta) superfamily member, is a p53 target gene that inhibits tumor cell growth via TGF-beta signaling pathway. Proc Natl Acad Sci U S A. 2000; 97:109–114. [PubMed: 10618379]
49. Shim M, Eling TE. Protein kinase C-dependent regulation of NAG-1/placental bone morphogenic protein/MIC-1 expression in LNCaP prostate carcinoma cells. J Biol Chem. 2005; 280:18636–18642. [PubMed: 15757899]
50. Zimmers TA, Gutierrez JC, Koniaris LG. Loss of GDF-15 abolishes sulindac chemoprevention in the ApcMin/+ mouse model of intestinal cancer. J Cancer Res Clin Oncol. 2010; 136:571–576. [PubMed: 19784846]
51. Gitenay D, Baron VT. Is EGR1 a potential target for prostate cancer therapy? Future Oncology. 2009; 5:993–1003. [PubMed: 19792968]
52. Baron V, Adamson ED, Calogero A, Ragona G, Mercola D. The transcription factor Egr1 is a direct regulator of multiple tumor suppressors including TGF[beta]1, PTEN, p53, and fibronectin. Cancer Gene Ther. 2005; 13:115–124. [PubMed: 16138117]
53. Shureiqi I, Lippman SM. Lipoxygenase Modulation to Reverse Carcinogenesis. Cancer Res. 2001; 61:6307–6312. [PubMed: 11522616]

54. Shappell SB, Olson SJ, Hannah SE, Manning S, Roberts RL, Masumori N, et al. Elevated Expression of 12/15-Lipoxygenase and Cyclooxygenase-2 in a Transgenic Mouse Model of Prostate Carcinoma. Cancer Res. 2003; 63:2256–2267. [PubMed: 12727848]
55. Xu J, Kimball TR, Lorenz JN, Brown DA, Bauskin AR, Klevitsky R, et al. GDF15/MIC-1 Functions As a Protective and Antihypertrophic Factor Released From the Myocardium in Association With SMAD Protein Activation. Circ Res. 2006; 98:342–350. [PubMed: 16397142]
56. Seeler J-S, Dejean A. Nuclear and unclear functions of SUMO. Nat Rev Mol Cell Biol. 2003; 4:690–699. [PubMed: 14506472]
57. Felin J, Mayo J, Loos T, Jensen JD, Sperry D, Gaufin S, et al. Nuclear variants of bone morphogenetic proteins. BMC Cell Biol. 2010; 11:20. [PubMed: 20230640]
58. Lindeman GJ, Gaubatz S, Livingston DM, Ginsberg D. The subcellular localization of E2F-4 is cell-cycle-dependent. Proc Natl Acad Sci U S A. 1997; 94:5095–5100. [PubMed: 9144196]
59. Sharma M, Jamieson C, Johnson M, Molloy MP, Henderson BR. Specific Armadillo Repeat Sequences Facilitate beta-Catenin Nuclear Transport in Live Cells via Direct Binding to Nucleoporins Nup62, Nup153, and RanBP2/Nup358. J Biol Chem. 2012; 287:819–831. [PubMed: 22110128]
60. Wang YN, Yamaguchi H, Huo L, Du Y, Lee HJ, Lee HH, et al. The translocon Sec61beta localized in the inner nuclear membrane transports membrane-embedded EGF receptor to the nucleus. J Biol Chem. 2010; 285:38720–38729. [PubMed: 20937808]
61. Joshi JP, Brown NE, Griner SE, Nahta R. Growth differentiation factor 15 (GDF15)-mediated HER2 phosphorylation reduces trastuzumab sensitivity of HER2-overexpressing breast cancer cells. Biochem Pharmacol. 2011; 82:1090–1099. [PubMed: 21803025]
62. Janknecht R, Wells NJ, Hunter T. TGF-β-stimulated cooperation of Smad proteins with the coactivators-CBP/p300. Gene Dev. 1998; 12:2114–2119. [PubMed: 9679056]
63. Massagué J, Seoane J, Wotton D. Smad transcription factors. Gene Dev. 2005; 19:2783–2810. [PubMed: 16322555]
64. Lönn P, van der Heide LP, Dahl M, Hellman U, Heldin C-H, Moustakas A. PARP-1 Attenuates Smad-Mediated Transcription. Mol Cell. 2010; 40:521–532. [PubMed: 21095583]
65. Alarcón C, Zaromytidou A-I, Xi Q, Gao S, Yu J, Fujisawa S, et al. Nuclear CDKs Drive Smad Transcriptional Activation and Turnover in BMP and TGF-β Pathways. Cell. 2009; 139:757–769. [PubMed: 19914168]
66. Turner JG, Dawson J, Sullivan DM. Nuclear export of proteins and drug resistance in cancer. Biochem Pharmacol. 2012; 83:1021–1032. [PubMed: 22209898]
67. Trapnell C, Roberts A, Goff L, Pertea G, Kim D, Kelley DR, et al. Differential gene and transcript expression analysis of RNA-seq experiments with TopHat and Cufflinks. Nat Protoc. 2012; 7:562–578. [PubMed: 22383036]
68. Inui M, Manfrin A, Mamidi A, Martello G, Morsut L, Soligo S, et al. USP15 is a deubiquitylating enzyme for receptor-activated SMADs. Nat Cell Biol. 2011; 13:1368–1375. [PubMed: 21947082]

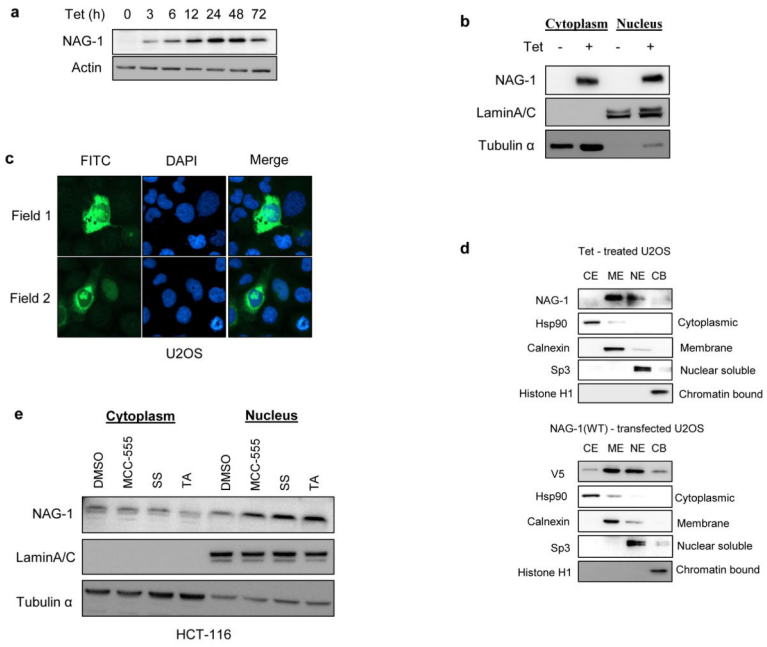

Figure 1.

NAG-1 expression observed in the nuclear fraction. (**a**) Western blot analysis of tetracycline-inducible U2OS cells. Cells grown in *tet*-free FBS were treated with 2 μg/mL tetracycline for the indicated times. Actin antibody was used for the loading control. (**b**) Nuclear and cytoplasmic expression of NAG-1. Cytoplasm and nuclear fractions of inducible U2OS cells were isolated after stimulation with 2 μg/mL tetracycline for 24 h. Expression of NAG-1, lamin A/C (nuclear marker), and tubulin α (cytoplasmic marker) were analyzed by Western blot. (**c**) U2OS cells transfected with GFP-tagged NAG-1 (WT) were fixed and analyzed by immunofluorescence with antibodies against GFP as described in the Materials and Methods section. DAPI was used to stain the nuclei. Two independent fields are shown. (**d**) Tetracycline-induced U2OS (top panel) and wild-type U2OS cells transfected with NAG-1/V5/His expression vector (bottom panel) were subjected to subcellular fractionation, and Western blot was performed. CE, cytoplasmic extract; ME, membrane extract; NE, nuclear extract; CB, chromatin-bound extract. Markers in each fraction are shown. Sp3 exhibits multiple bands, and a 78 kDa band is shown. (**e**) HCT-116 cells were treated with 10 μM of each compound for 24 h and subjected to Western blot analysis. MCC-555 is a PPARγ ligand, whereas SS (sulindac sulfide) and TA (tolfenamic acid) are NSAIDs. DMSO was used for a vehicle.

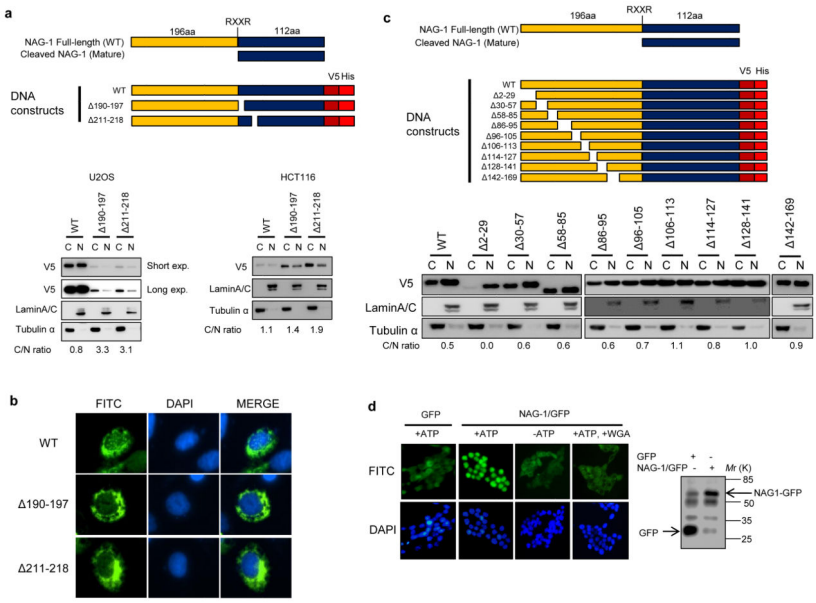

Figure 2.

NAG-1 moves to the nucleus through a nuclear pore complex in an energy-dependent manner. (**a**) Schematic diagrams of plasmids encoding different truncated forms of NAG-1, Δ190-197, and Δ211-218. Deletion sequences are presented in the bottom panel. Pro-NAG-1 (Wild-type) is designated at the top: propeptide (yellow), mature peptide (blue), followed by V5 epitope and histidine track (red). C, cytoplasmic and N, nuclear fractions of U2OS (bottom left panel) and HCT-116 (bottom right panel) cells transfected with either WT or two mutant clones were subjected to Western blot. Antibodies against lamin A/C and Tubulin α were used for nuclear and cytoplasm markers, respectively. Intensity ratio for cytoplasmic to nuclear (C/N) expression is shown at the bottom. (**b**) Immunofluorescence assay with antibodies against V5 from WT and two mutant NAG-1-transfected U2OS cells. DAPI was used for staining nuclei. Representative fields are shown. (**c**) Schematic diagram of serial deletion mutants of NAG-1. HCT-116 cells were transfected with each mutant clone as described in the Materials and Methods section, and Western blot analysis was performed using C and N fractions. Intensity ratio for C/N expression is shown at the bottom. (**d**) *In vitro* nuclear import assays of NAG-1/GFP protein. HCT116 cells were permeabilized with digitonin (30 ng/ml) for 5 min and then incubated in a reaction buffer containing cytosol extract and ATP regeneration system with either NAG-1/GFP or GFP protein. For WGA treatment, permeabilized cells were pre-incubated with 0.05 mg/mL WGA for 30 min at room temperature and incubated for 30 min at 37°C with complete reaction buffer. The cells were washed with reaction buffer and then fixed and stained with DAPI. The cells were viewed by fluorescence microscopy. Right panel, expression of in vitro translated GFP and NAG-1/GFP by Western blot.

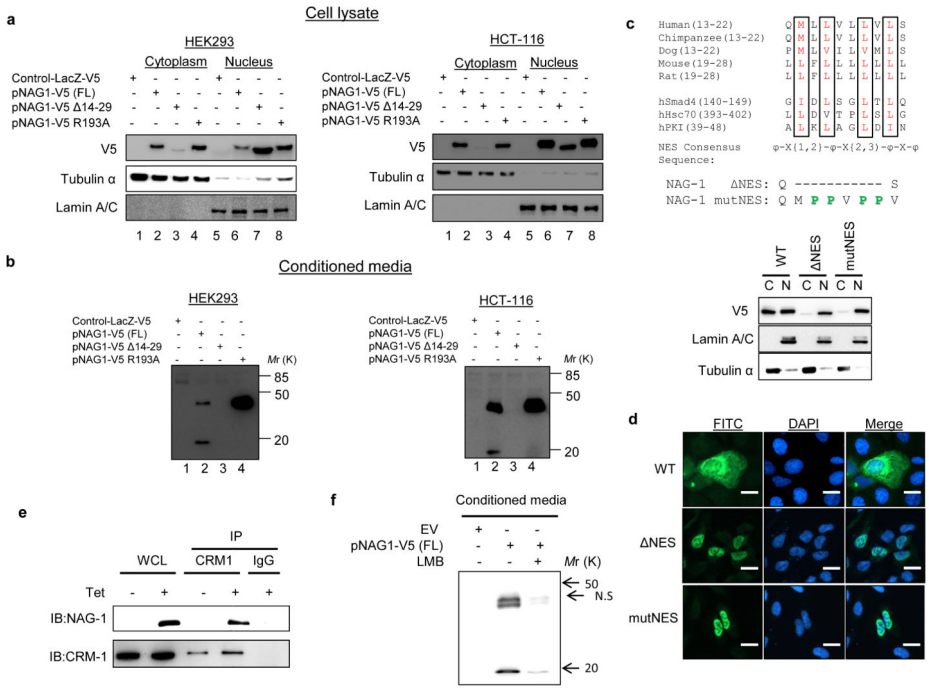

Figure 3.

A canonical nuclear export signal (NES) of NAG-1 contributes predominant nuclear expression of NAG-1. (**a**) HEK293 (left panel) and HCT-116 (right panel) cells were transfected with either control LacZ vector, full-length pNAG-1-V5-WT (FL), or the two mutant clones pNAG-1-V5 Δ14-29 and pNAG-1-V5 R193A. Then the cytoplasm and nuclear fractions were isolated. Western blot analysis was performed against V5, tubulin α, and lamin A/C. (**b**) Conditioned media from (**a**) were harvested and concentrated by Corning concentrations (10 kDa MWCO), and 30 μL concentrated conditioned media was analyzed by Western blot with anti-V5 antibody. (**c**) A putative NES in the N-terminal domain of NAG-1. The putative NES sequence in human NAG-1 is aligned with NAG-1 in other species, and also compared with the known NES sequences in Smad4, Hsc70, and PKI. Two mutant NAG-1 clones, ΔNES and mutNES, are shown. U2OS cells were transfected with the indicated vectors. Nuclear, N, and cytoplasmic, C, fractions were analyzed using the indicated antibodies as shown at bottom. (**d**) U2OS cells were transfected with WT, ΔNES, or mutNES NAG-1-expressing vectors, and immunofluorescence assay was performed with antibodies against V5 (green) with DAPI staining (blue). Scale bars, 10 μm. (**e**) *Tet*-inducible U2OS cells were treated with 2 μg/mL tetracycline for 24 h, and cell lysates were isolated with a modified RIPA buffer as described in the Materials and Methods section. The cell lysates were incubated overnight with 2 μg CRM1 or normal IgG antibodies, subjected to immunoprecipitation for 3 h, and then subjected to Western blot analysis using NAG-1 or CRM1 antibodies. The whole cell lysate (WCL) was loaded with 30 μg. (**f**) U2OS cells were transfected with pNAG-1/V5/His WT for 6 h, then 10 nM LMB added for 18 h. Conditioned media from the cells was subjected to Western blot analysis.

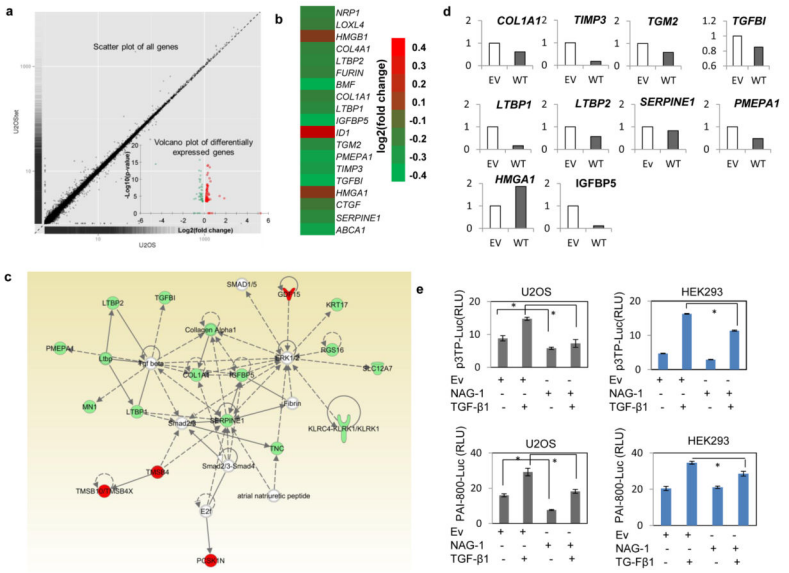

Figure 4.

NAG-1 modulates TGF-β signaling at the transcriptional level. (**a**) The scatter plot from RNA-seq data compares the expression of inducible U2OS cells with or without tetracycline. The straight line highlights the general similarities between the two conditions, with the volcano plot (red for up-regulation, green for down-regulation) showing the differentially expressed genes (Supplementary Table 2). (**b**) Heat map representation of the mRNA expression profile showing changes in TGF-β downstream target genes between U2OS and tetracycline-treated U2OS cells. Gene expression data were log2 transformed and then normalized prior to generating the heat map for direct comparison of data. Differential expression for each cell is presented. (**c**) Schematic representation of Ingenuity network analysis. Gene symbols are in red and green for up- and down-regulation, respectively. Dashed lines show indirect interactions, while continuous lines represent direct interactions, based on Ingenuity's knowledgebase. (**d**) Real-time PCR of selected genes from the heat map. Empty vector (EV) or wild-type (WT) NAG-1 was transfected into U2OS cells and total RNAs isolated; then qRT-PCR was performed as described in the Materials and Methods section. The data were normalized by the expression of the housekeeping Ribosomal Protein, Large, P0 (RPLP0) mRNA, and further normalized to the level of the empty vector transfected group, which was set at 1. (**e**) Two reporter genes, *p3TP-Luc* and *pPAI-800-Luc* (*SERPINE1 promoter*), were co-transfected with either empty vector or NAG-1-expressing vector into U2OS and HEK293 cells that exhibited an intact TGF-β signaling pathway. Transfected cells were treated with TGF-β1 (10 ng/mL for 24 h), and luciferase activity was measured. The graph shows mean values with ± SD from three replicates. $*P < 0.05$, compared to NAG-1 transfected cells.

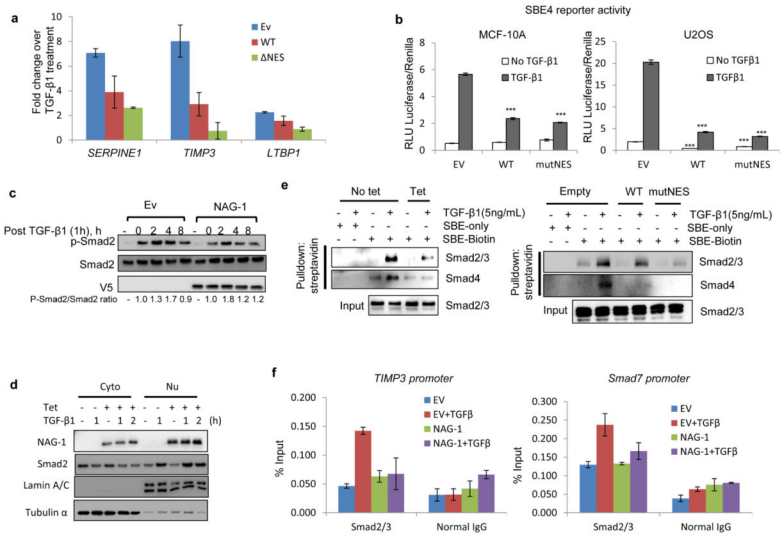

Figure 5.

Nuclear NAG-1 interrupts DNA binding activity of the Smad complex. (**a**) Real-time PCR for expression of *SERPINE1*, *TIMP3*, and *LTBP1* genes in the presence of TGF-β1. U2OS cells were transfected with empty (EV), wild-type NAG-1 (WT), or ΔNES NAG-1-expression vectors. Cells were treated with TGF-β1 (2 ng/mL) for 12 h, and gene expression was analyzed by qRT-PCR as described in the Materials and Methods section. The graph shows mean values of fold changes over TGF-β1 treatment. (**b**) Wild-type NAG-1 and mutNES-NAG-1 expression decreased Smad binding element (SBE)-containing promoter activity. MCF-10A and U2OS cells were transfected with SBE4 reporter and indicated expression vectors. Cells were treated with TGF-β1 (10 ng/mL) for 24 h and luciferase activity measured. The graph shows mean values ± SD from three replicates. ***$P < 0.001$, compared to empty vector-transfected cells. (**c**) U2OS cells were transfected with either empty or wild-type NAG-1 expression vector. After treatment with TGF-β1 (2 ng/mL) for 1 h, the media were replaced with fresh media, and cell lysates were isolated at the indicated time points. Whole cell lysates (30 μg) were subjected to Western blot analysis using phosphor-Smad2, and Smad2 antibodies. (**d**) *Tet*-inducible U2OS cells were stimulated with TGF-β1 (2 ng/mL) for the indicated time points, and then cell lysates were subjected to nuclear and cytoplasmic fractionation followed by Western blot with the indicated antibodies. Lamin A/C and tubulin α were used as nucleus and cytoplasm markers, respectively. (**e**) DNA pull-down and Western blot with anti-Smad2/3 and anti-Smad4 antibodies. Cell lysates from either U2OS or U2OS-tet cells were incubated with SBE oligo DNA as described in the Materials and Methods section. SBE-bound proteins were reduced in U2OS-tet compared to U2OS (left panel), and similar results were obtained using ectopic NAG-1 expression vectors into U2OS cells (right panel). (**f**) *In vivo* binding of Smad2/3 to the TIMP3 or Smad7 promoter in U2OS cells stimulated with TGF-β1 (2 ng/mL) using the ChIP assay. Inducible U2OS cells were stimulated by tetracycline for 24 h (left panel), and wild-type U2OS cells were transfected with either empty vector or NAG-1 expressing vector (right panel). The ChIP assay for endogenous smad2/3 indicates enhanced recruitment of Smad2/3 to the TIMP3 or Smad7 promoter region after simulation with TGF-β1 for 3 h and decreased occupancy on these promoter regions by NAG-1 expression.

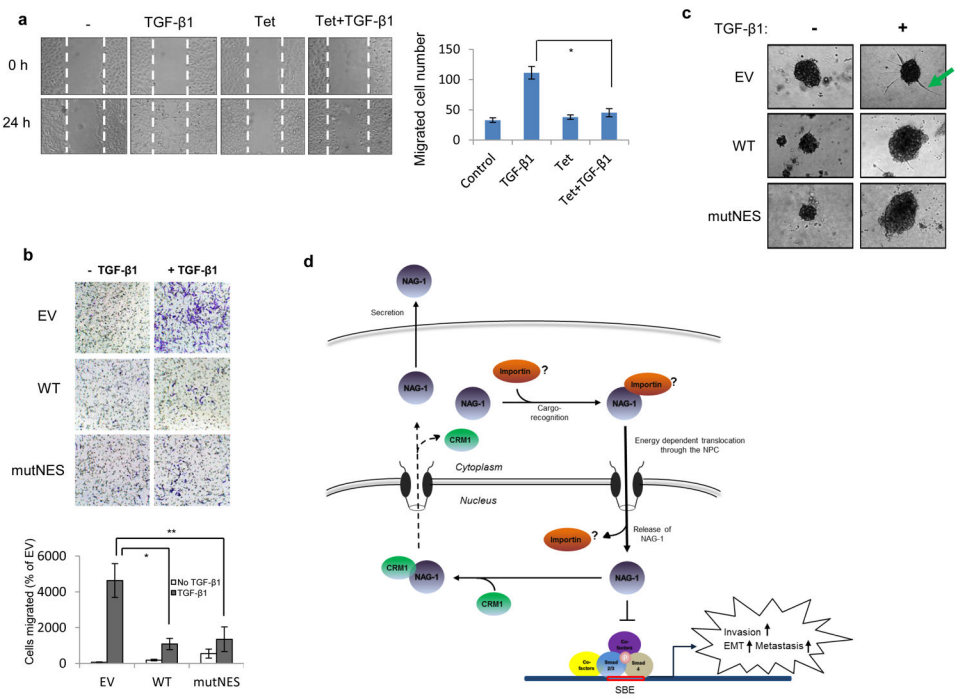

Figure 6.

NAG-1 blocks TGF-β1-induced cell migration/invasion. (**a**) Cell migration assay. *Tet*-inducible U2OS cells were scratched with a pipet tip, and images were taken at 0 and 24 h by phase-contrast microscopy as the cells repopulated the wound. To measure the rate of healing, the area between the wound edges was measured and compared relative to the area of the original wound at t = 0. Dotted lines represent the original wound area. The graph (right panel) shows mean values with ± SD from three replicates (**P* < 0.05). (**b**) Transwell migration assay. Transwell chambers were used to verify migration potential. U2OS cells transfected with the indicated vector were incubated with 10 ng/mL TGF-β1 for 18 h. Cells attached in the lower chamber were stained with crystal violet and counted under a light microscope. The graph shows mean ± SD of three independent experiments (**P* < 0.05 and ***P* <0.01). (**c**) U2OS cells transfected with either empty, wild-type NAG-1, or mutNES NAG-1 were prepared and subjected to an *in vitro* 3-D spheroid cell invasion assay as described in the Materials and Methods section. The green arrow indicates cells invading the surrounding invasion matrix. (**d**) A proposed model for nuclear-cytoplasmic shuttling and the function of NAG-1 in the nucleus. Cytoplasmic NAG-1 is recognized by import machinery and enters the nucleus via the NPC in an energy-dependent manner. In the nucleus, NAG-1 interrupts the DNA binding capacity of the Smad complex giving rise to attenuation of Smad signaling. Nuclear NAG-1 interacts with CRM1 for export out of the nucleus. NAG-1 is secreted by an unknown secretory pathway and likely binds to an unidentified receptor.